Eksploatacja i Niezawodnosc - Maintenance and Reliability
Volume 29 (2027), Issue 1
https://ein.org.pl
The Polish Maintenance Society

Optimization-based maximum power point tracking for wind energy systems: a comparative study of gray wolf and whale algorithms

Hasan Bektas Percin[1,*], Abuzer Caliskan[1]

[1] Electrical Electronics Engineering, Firat University, Turkey
* Corresponding Author: hbpercin@firat.edu.tr

Received: 7 April 2026
Revised: 19 April 2026
Accepted: 30 April 2026
Online: 9 July 2026

Abstract

Maintaining high energy conversion efficiency under varying wind conditions remains a major challenge in wind energy systems. To address this issue, maximum power point tracking (MPPT) techniques have been widely employed Traditional methods frequently depend on precise system parameters or fixed control structures, which may lead to performance degradation. Conversely, optimization-based algorithms can operate under more favorable conditions without requiring specific structures. In this study, two metaheuristic algorithms, the Gray Wolf Optimizer (GWO) and Whale Optimization Algorithm (WOA), were implemented as MPPT controllers in the MATLAB/Simulink environment. The main contribution of this study is the evaluation of two metaheuristic optimization algorithms and provision of practical insights into their suitability for wind energy systems. The simulation results showed that the GWO-based method outperformed its WOA counterpart, achieving a higher tracking efficiency of 98.2% and a lower oscillation rate (<2%), indicating higher effectiveness under dynamic wind conditions.

Keywords: *wind energy, MPPT, metaheuristic optimizations, MATLAB/Simulink, energy efficiency*

Article citation:
Percin H B, Caliskan A, Optimization-based maximum power point tracking for wind energy systems: a comparative study of gray wolf and whale algorithms, Eksploatacja i Niezawodnosc – Maintenance and Reliability 2027: 29(1) http://doi.org/10.17531/ein/221284

Highlights

- MPPT strategies provide energy efficiency and system durability.
- Comparison of different optimization methods for wind energy systems.
- Simulation application in the MATLAB/Simulink environment.
- Better performance than traditional MPPT methods.

1. Introduction

Concerns regarding the detrimental effects of fossil fuels and global warming have prompted a shift in energy policies towards the adoption of renewable energy sources [1,2]. Wind energy stands out among these resources because of its abundance, cost-effectiveness, and environmentally friendly nature [3]. However, its intermittent and variable characteristics lead to output fluctuations under changing operating conditions, requiring maximum power point tracking (MPPT) techniques to maximize energy capture, improve cost efficiency, and extend system lifespan [4]. MPPT techniques regulate the operating speed of wind energy conversion systems to continuously track changes in wind speed and maintain optimal energy extraction.

MPPT implementation involves several challenges, including maintaining efficiency, mitigating environmental impacts, ensuring system stability, and addressing implementation complexity. Consequently, researchers and engineers continue to develop innovative solutions to overcome these challenges. Various MPPT methods have been extensively investigated in the literature and are generally classified into direct, indirect, intelligent, and hybrid approaches. Indirect approaches incorporate methods such as the tip-speed ratio (TSR), optimal torque (OT), and power signal feedback (PSF) algorithms [5–9]. These methods rely on the characteristics of wind turbines. However, direct control approaches do not

require prior system knowledge and use techniques such as Perturb and Observe (P&O), Incremental Conductance (INC), and Optimum Relation-Based (ORB) MPPT algorithms [10–12]. The aforementioned methods have demonstrated effective MPP tracking performance for wind energy conversion systems (WECSs). However, each approach has inherent limitations and drawbacks. Therefore, developing a highly accurate and reliable MPPT algorithm remains a significant challenge [13–15].

MPPT control can be executed using direct or indirect approaches. However, these methodologies may suffer from reduced effectiveness owing to the inherent nonlinearity of the system [5,6,16,17]. Moreover, the need for additional devices can increase the overall system cost. Consequently, intelligent algorithms have emerged as a promising alternative to overcome these limitations. They employ a variety of computational techniques to improve system performance. The term "intelligent" refers to their high adaptability and ability to operate independently of system characteristics. Intelligent control algorithms include fuzzy logic controllers (FLC) [18–21], artificial neural networks [22–25], and metaheuristic optimization algorithms. A range of metaheuristic optimization algorithms with various parameters and modifications have been proposed for complex, nonlinear, and discontinuous problems. Inspired by natural phenomena or physical laws, these algorithms navigate nonlinear and discontinuous solution spaces and explore them using diverse strategies to find optimal or near-optimal solutions [26–30]. Various optimization algorithms, such as particle swarm optimization (PSO), genetic algorithm (GA), bat optimization (BO), artificial bee colony (ABC), and cuckoo search algorithm, have also been proposed as control techniques for various renewable energy sources [31–34]. In addition to these methods, hybrid approaches that combine two or more MPPT techniques have been developed to overcome the inherent limitations of individual algorithms [3,10,35–40].

Although a wide range of MPPT control strategies have been proposed for WECSs, there is a notable gap in the literature regarding the comparative evaluation of optimization-based algorithms for MPPT control. The Grey Wolf Optimizer (GWO) and Whale Optimization Algorithm (WOA) have gained attention in renewable applications. Their efficiency and simplicity have positioned these approaches at the forefront of solving several engineering problems [41–43]. This study presents a comparative evaluation of these MPPT methods for maximizing energy extraction from WECSs under varying wind conditions. Simulations were performed using specific wind profiles, and the algorithms were evaluated based on key performance indicators, including tracking efficiency, response time, power stability, and adaptability. To assess the effectiveness of the proposed metaheuristic algorithms, their performance was benchmarked against conventional control methods widely reported in the literature. The remainder of this paper is organized as follows: Section 2 presents the fundamental principles of WECSs and their components, along with explanations of metaheuristic algorithms. Section 3 presents the simulation results of the proposed methods using MATLAB/Simulink. The conclusions are presented in the final section.

2. Material and method

WECSs comprise components that capture the kinetic energy of the wind and convert it into usable electrical energy through successive mechanical and electrical energy conversion processes. The energy conversion scheme of WECSs is shown in Figure 1.

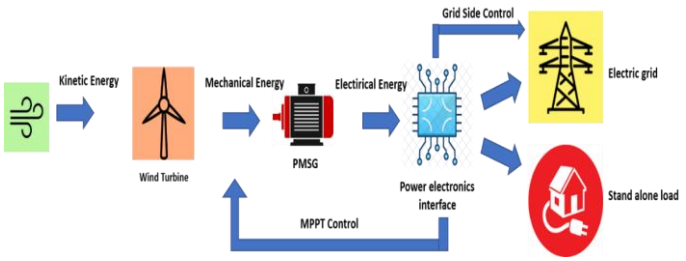

Figure 1. Basic working scheme of a WECS.

Wind turbines (WTs) play a pivotal role in converting kinetic energy into mechanical energy. WTs are generally classified into horizontal-axis (HAWTs) and vertical-axis (VAWTs) types. HAWTs are more common owing to their simple configuration, efficiency, and long service life. Permanent magnet synchronous generators (PMSGs) offer significant advantages for direct-drive energy generation by eliminating the need for a gearbox, thereby reducing maintenance costs and overall losses. Finally, the generated energy is delivered to either the grid or a stand-alone load via power electronic interfaces. These interfaces are implemented

as power converter units in various configurations, depending on factors such as power level, control objectives, and cost-effectiveness. MPPT strategies are integrated into these interfaces to ensure efficient and stable system operation [44].

2.1. WECS modelling

To analyze and design suitable control techniques for various WECS control objectives, the basic WECS parameters must be mathematically expressed. The mechanical power (P_M) produced by a wind turbine is expressed as in Equation (1).

$$P_M = \frac{1}{2} \times C_P \times p \times A \times {V_W}^3 \quad (1)$$

In Equation (1), A represents the area swept by the turbine blades, p denotes the air density, typically taken as a constant value of 1.225 kg/m³, and V_W signifies the instantaneous wind speed. C_P stands for the power coefficient, serving as a measure of the efficiency of energy conversion [45]. In MPPT control, the primary goal is to maintain this coefficient within an optimal range. This coefficient is derived as a function of the tip-speed ratio (λ) and pitch angle (β), as expressed in Equation (2).

$$C_P(\lambda, \beta) = C_1 \left(\frac{C_2}{\lambda_i} - C_3 \times \beta - C_4 \right) e^{-(C_5/\lambda_i)} + C_6 \times \lambda \quad (2)$$

$C_{(1\text{-}6)}$ are characteristic values for turbine designs. β (pitch angle) is adjusted to prevent the turbine from damage especially at higher wind speeds. The coefficients $C_{(1\text{-}6)}$ are used to approximate the power coefficient curve. In this study, the commonly used parameter values reported in [45] are adopted as C_1=0.5176, C_2=116, C_3=0.4, C_4 =5, C_5 =21, and C_6=0.0068. These coefficients are widely used to represent the aerodynamic behavior of variable speed wind turbines. The tip speed ratio (λ) and λ_i parameters in Equation (2) are defined as shown in Equation (3).

$$\lambda = \frac{w \times R}{V_W}, \quad \frac{1}{\lambda_i} = \frac{1}{\lambda + 0.08\beta} - \frac{0.035}{\beta^3 + 1} \quad (3)$$

In Equation (3), R is the radius of the area swept by the turbine blades and ω is the mechanical speed of the WECS (rad/s). The relationship between Cp and λ based on various beta (angle) values for a specific wind speed is illustrated in Figure 2. Typically, the pitch angle is set to a minimum value below the nominal wind speed. Consequently, C_p depends only on λ. Figure 2 shows that the power coefficient (Cp) and maximum power are attained at a specific value of the tip-speed ratio (λ), referred to as the optimum tip-speed ratio (λ_{opt}).

The tip speed ratio (λ) can be regulated by adjusting the mechanical speed (ω) in response to variations in wind speed, as expressed in Equation (3). Maintaining the power coefficient at its optimal value (C_{p_opt}) by regulating the mechanical speed and tip speed ratio is the fundamental principle of MPPT control in WECSs [45,46]. To achieve these objectives, different control strategies must be implemented across the operating regions defined by the wind speed ranges of WECSs. The four primary operating regions are illustrated in Figure 3.

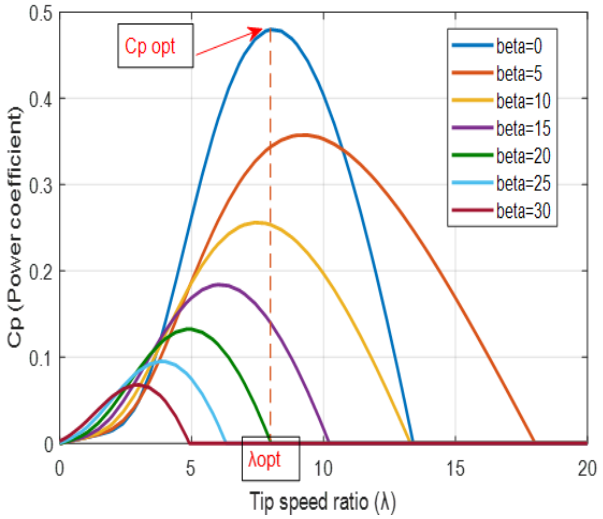

Figure 2. Variation of C_p with λ at different angle values.

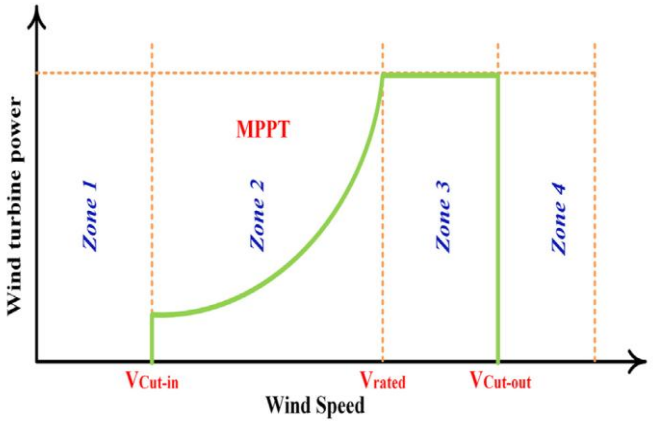

Figure 3. The operating regions of the WECS.

The operational limits of wind speed in Figure 3 are defined by the cut-in ($V_{Cut\text{-}in}$) and cut-out ($V_{Cut\text{-}out}$) wind speeds. The wind turbine is configured to automatically shut down beyond these thresholds. When the wind speeds range between $V_{Cut\text{-}in}$ and rated values (V_{Rated}), the MPPT controller is activated by adjusting the rotational speed and setting the pitch angle of the turbine blades to a minimum value [47–49]. Based on this operating principle, the relationship between the mechanical

output power (P_m) and mechanical (rotor) speed at different wind speeds is illustrated in Figure 4.

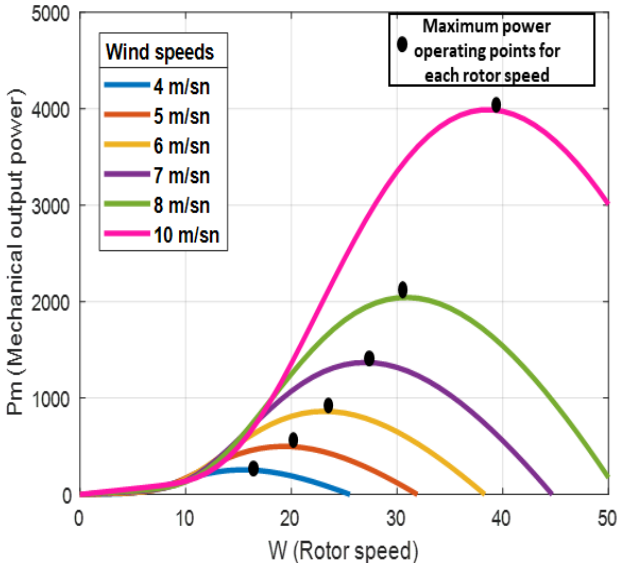

Figure 4. Mechanical output power variation at different wind speeds.

Each wind speed in Figure 4 generates a distinct power curve. The objective of the MPPT controller is to adjust the rotor speed to maintain the operating points of the system at the maximum power value for varying wind speeds.

2.2. Power electronic interface

MPPT controllers are implemented using power-electronic interfaces. Many different configurations have been used in the literature for energy conversion systems [45,50]. This study utilized an interface incorporating a rectifier integrated with a boost converter, which offers advantages such as compactness, high reliability, and ease of controllability. A circuit diagram of the proposed interface is presented in Figure 5.

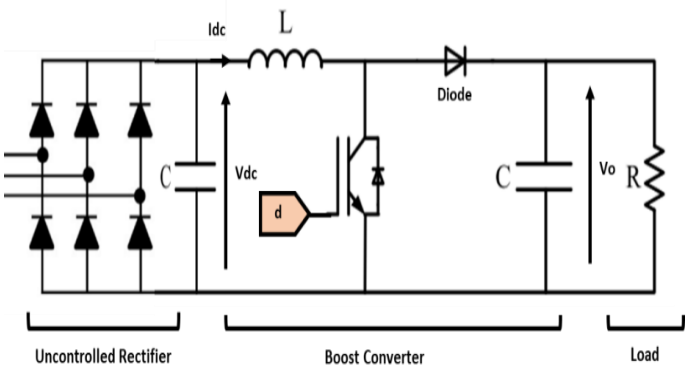

Figure 5. The diagram of the proposed interface.

In the circuit diagram, the rectifier converts the variable-frequency AC output into a DC power. This rectifier is followed by a boost converter, which adjusts the DC output voltage level and facilitates the implementation of the MPPT algorithm by dynamically regulating the duty cycle (d) to track the maximum power point (MPP). the relationship between the output voltage (Vo), the input voltage (Vdc), input current (Idc), and output current (Io) for a boost converter, is defined by Equation (4) and Equation (5) [45, 51].

$$V_o = \frac{V_{dc}}{1-d} \tag{4}$$

$$I_o = I_{dc} \times (1-d) \tag{5}$$

According to Equation (4), the adjustment of the duty cycle enables the control of the input and output parameters of the boost converter. The relationship between the input resistance (R_i) and output load resistance (R) is expressed as in Equation (6).

$$R_i = R \times (1-d)^2 \tag{6}$$

Based on Equation (6), a change in the input resistance can alter the output current and electromagnetic torque, thereby affecting the rotor speed. Thus, adjusting the duty cycle enables MPPT control by regulating the system speed. The effectiveness of this control strategy also depends on the proper design of the boost converter. In addition to the control principle, the appropriate calculation and selection of the converter parameters directly affect the dynamic response, efficiency, and power quality of the system. These parameters include the switching frequency (f_s), inductance (L), and capacitance (C) of the boost converter [45,51]. Incorrect sizing of these parameters can lead to power loss, inefficient tracking, and system failures.

2.3. Grey Wolf Optimization

The Grey Wolf Optimization (GWO) algorithm is a metaheuristic algorithm inspired by the hierarchical order and hunting behavior of grey wolf packs. The pack is organized by a leader named Alpha (α); this wolf is supported by another group member called Beta (β), who supports the leadership of the Alpha and also has the potential to replace the leader in the pack. The other members of the group are named Delta (δ) and Omega (ω), which obey other dominant wolves [52–54]. To evaluate the GWO algorithm, the most optimal solution is identified as alpha. Subsequently, the next two best solutions are defined as beta (β) and delta (δ). These wolves lead the pack, guiding the rest of the members, known as omega, in their

hunting behavior. In the first stage, the wolves surround their prey during the hunt. This behavior is expressed in Equations (7-8).

$$D = C \times \left(X_p(t) - X(t)\right) \quad (7)$$

$$X(t+1) = \left(X_p(t) - A \times D\right) \quad (8)$$

In Equations (7-8), t is the current iteration, A and C are coefficiency values, X_p is the prey position, and X represents the grey wolf position. A and C are vectorial values, which are determined as in Equation (9).

$$A = (2a) \times (r_1) - (a),\ C = 2 \times (r_2) \quad (9)$$

$$D_{alpha} = C_1 \times \left(X_{alpha}(t) - X(t)\right) \quad (10)$$

$$D_{beta} = C_2 \times \left(X_{beta}(t) - X(t)\right) \quad (11)$$

$$D_{delta} = C_2 \times \left(X_{delta}(t) - X(t)\right) \quad (12)$$

$$X_1 = \left(X_{alpha}(t) - A_1 \times D_{alpha}\right) \quad (13)$$

$$X_2 = \left(X_{beta}(t) - A_2 \times D_{beta}\right) \quad (14)$$

$$X_3 = \left(X_{delta}(t) - A_3 \times D_{delta}\right) \quad (15)$$

$$X(t+1) = \frac{X_1 + X_2 + X_3}{3} \quad (16)$$

The a value in Equation (9) decreases linearly from 2 to 0 throughout the iterations, whereas *r1* and *r2* are randomly generated vectors within the interval [0, 1]. The coefficients A and C determine the exploration and exploitation capabilities of the algorithm. The alpha, beta, and delta wolves represent the three best candidate solutions and guide the remaining wolves during the search process. Their position update mechanism is described by Equations (10–16). The distances between each search agent ($D_{alpha}, D_{beta}, D_{delta}$) and the three leading wolves are calculated, whereas Equations (13–16) update the wolves' positions based on these leaders (X_1, X_2, X_3) [47]. As the value of a decreases, the search gradually shifts from exploration to exploitation. The coefficient A varies within the range [−2a,2a], where $|A|<1$ promotes exploitation around the prey, while $|A|>1$ encourages exploration by moving search agents away from the current best solutions. The assigned C value is utilized to optimize GWO stages (exploration, exploitation) through all the iterations [53]. The optimization flowchart is shown in Figure 6.

The process shown in Figure 6 is repeated through all iterations. The GWO algorithm is characterized by its simplicity, adaptability, and effective global search capability, which helps prevent premature convergence to local optima.These attributes make it highly effective for tackling nonlinear and dynamic optimization problems, such as MPPT control.

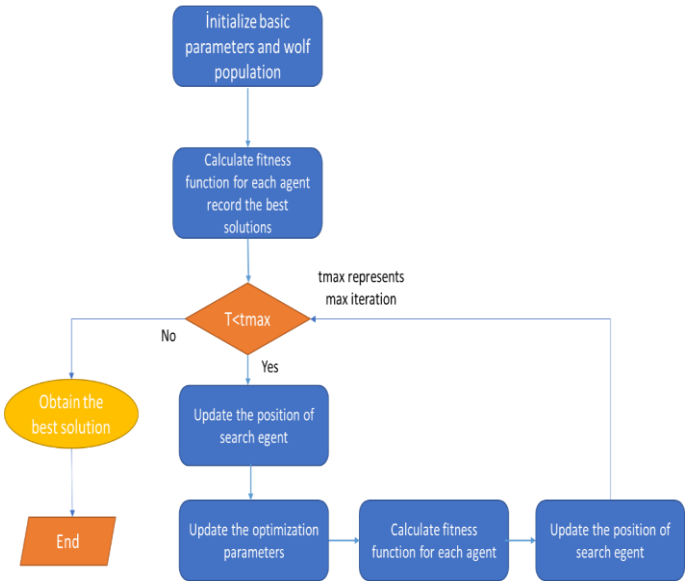

Figure 6. The optimization process of GWO.

2.4. Whale Optimization Algorithm

The Whale Optimization Algorithm (WOA) simulates the hunting behavior of humpback whales using a bubble-net hunting strategy. In nature, humpback whales engage in bubble-net feeding by diving to a certain depth beneath a school of fish and creating bubble spirals while swimming upward in a helical pattern, effectively trapping their prey in a shrinking circle [54,55]. This strategy is depicted in Figure 7.

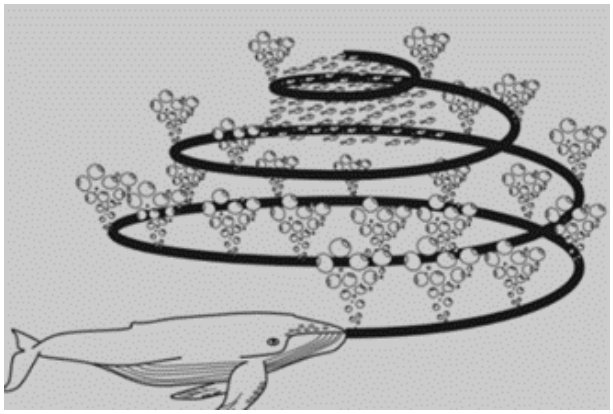

Figure 7. Bubble-net hunting behavior.

The modeling process of the WOA is defined by the following equations:

$$X(t+1) = (X_{rnd} - A \times D_{rnd}) \quad (17)$$

$$D_{rnd} = (C \times X_{rnd} - X(t))\ A > 1 \quad (18)$$

$$X(t+1) = (X^* - A \times D_{rnd}) \quad (19)$$

$$D = (C \times X^* - X(t))\ A < 1 \quad (20)$$

The positions of the whale (X) and prey (X^*) are key variables in Equations (17-20). The optimization process is organized into two stages: exploration (encircling) and

exploitation (spiral bubble-net attack). The transition between these stages is controlled by the parameter A. When $|A|>1$, the algorithm focuses on exploration, allowing the whale to search for food by randomly moving in the search space as expressed in Equation (17). For $|A|<1$, the whales create a spiral-shaped path around the prey, mimicking the bubble-net hunting behavior. The position update equation for this stage is expressed in Equation (19). The update and calculation of A, C, the distance to the optimal solution (D'), and the next iteration position X(t+1) are expressed as follows:

$$A = (2a) \times r - 2,\ a = 2 - 2\left(\frac{t}{tmax}\right) \quad (21)$$

$$C = 2 \times r \quad (22)$$

$$X(t+1) = (X^* + D' \times e^{bl} * \cos(2\pi l)) \quad (23)$$

$$D' = (X^* - X(t) \times D' \times e^{bl} * \cos 2\pi l) \quad (24)$$

$$l = (a_2 - 1) \times rnd + 1 \quad (25)$$

$$a_2 = (-1 - (\frac{t}{t_{max}})) \quad (26)$$

In Equations (21–26), the parameters are defined as follows: A is randomly adjusted within the range [−2,2], while "l" is a random constant in the interval [−1,1]. Similarly, rnd is a random variable distributed within [−1,1]. The parameters t and t_{max} denote the current and maximum iteration numbers, respectively, whereas b is a predefined constant within the range [0,10]. Finally, r is a uniformly distributed number within [0,1]. The proper configuration of these parameters enhances the convergence behavior and improves the robustness of the optimization process under varying operating conditions. The flowchart of the WOA is shown in Figure 8.

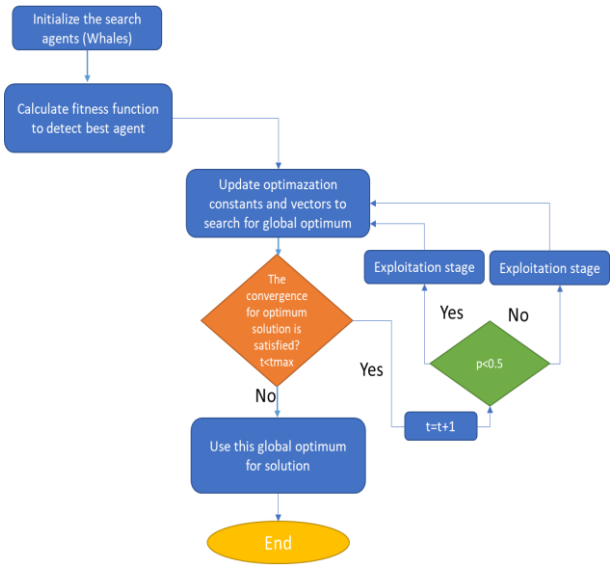

Figure 8. The flowchart of WOA.

Figure 8 illustrates a probability value, designated as "p" in this study, which represents the probability that whales exhibit a specific behavior during the optimization stages. The probability value determines the likelihood of two behaviors: spiraling around the target or direct hunting. This mechanism ensures balanced exploration and exploitation, preventing premature convergence and local optimum stagnation in multimodal search spaces.

3. Findings and discussion

Before proceeding to the simulation phase, the implementation framework of the optimization-based MPPT algorithms is presented in Figure 9. The proposed configuration illustrates the integration of these algorithms into the MPPT control scheme to maximize energy capture while maintaining system stability under varying wind conditions.

For the selected algorithms, the problem was defined as the process of searching for an optimal solution, guided by an objective function within a defined solution space, aiming to either minimize or maximize the function to effectively address the problem. The power value is calculated using the input current (Idc) and the input voltage (Vdc) of the boost converter. The (MPPT) control is performed by modulating the duty cycle (d) of the switching device in the boost converter. In both algorithms, the duty cycle serves as the population variable, whereas the power value represents the objective function. The duty cycle was constrained between 0.1–0.9. The iterations for both algorithms continued until the maximum power value was reached, or a specified termination criterion was met. Among the termination criteria, power variation tolerance (τ) is a critical parameter for implementing MPPT strategies. This parameter can be expressed as follows:

$$\frac{P_{n+1} - P_n}{P_n} \leq \tau \quad (27)$$

The power variation tolerance (τ) defines the acceptable range of (MPP) fluctuation in the output power and does not require further adjustment. The power variation tolerance (τ) could be defined between 5%-15% to adjust the control sensitivity. By tuning it, system designers can balance the tracking accuracy and system stability in real-time conditions. The parameters used for the WECS and optimization algorithms are listed in Table 1.

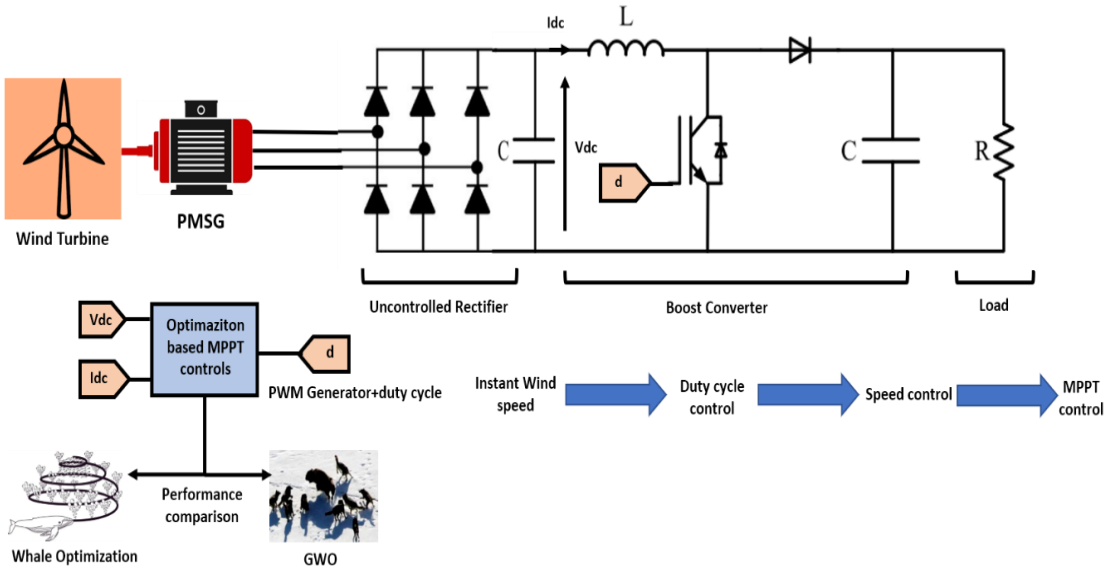

Figure 9. The overall control scheme of MPPT controls.

Table 1. Parameters of WECS and optimization algorithms.

WECS parameters		GWO parameters		WOA parameters	
Air density (p)	1.2 kg/m^3	Population (wolf) size	20	Population size	20
Turbine radius (R)	2 m	Iteration number	100	Iteration size	100
Rated wind speed	10 m/s	a (randomly adjusted coefficient)	0<a<2	a (randomly adjusted coefficient)	0<a<2
Optimal tip speed ratio (λ_{opt})	8.1	r (Random vector)	0<r<1	r (Random vector)	0<r<1
Optimal Power coefficient ($C_{p\ opt}$)	0.48			p value	0.5
Rated turbine power	4 kW				

Since both GWO and WOA are stochastic population-based algorithms, each simulation was repeated 30 times to minimize the effects of random initialization and improve the reliability of the results. The parameter settings listed in Table 1 were adopted from widely accepted configurations reported in the literature [53,56,57]. These values ensured optimal performance while maintaining consistency with previous studies. Simulations were performed for the variable wind speed model, as shown in Figure 10.

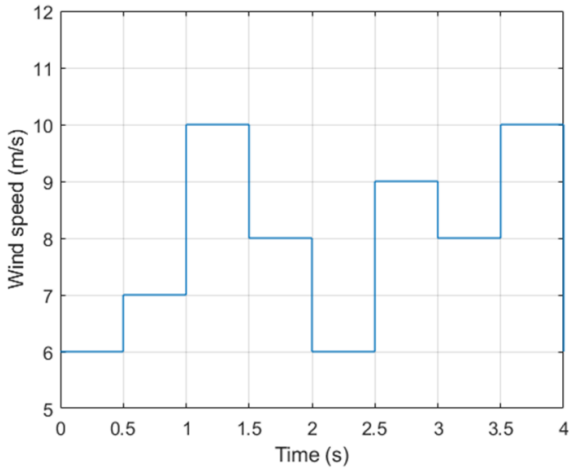

Figure 10. Variable wind speed profile.

The purpose of using the selected profile model was to test the responsiveness and robustness of the proposed MPPT-based control scheme under challenging operating conditions. For the proposed model, the variations in the turbine power coefficient (Cp) using each algorithm are shown in Figure 11.

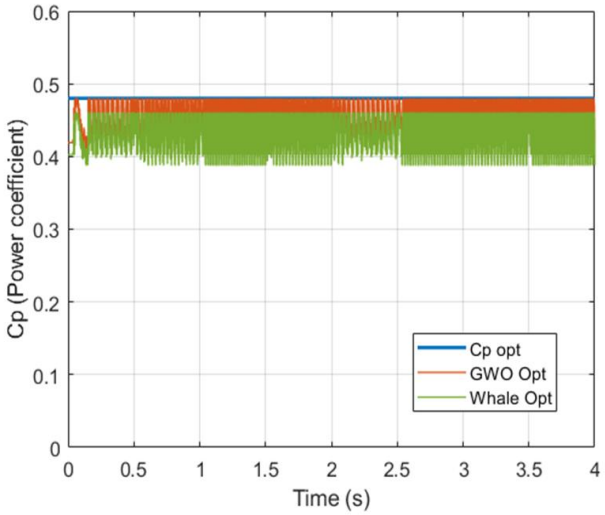

Figure 11. Power coefficient variations for the both algorithms.

In Figure 11, it can be seen that the proposed algorithms maintained the instant Cp values close to the optimal value of 0.48 (blue curve). The Cp waveform in the GWO algorithm

(orange curve) has fewer oscillations and exhibits more stable variations than that in the WOA (green curve). Furthermore, the Cp value of GWO is closer to the optimal value. The fluctuations observed in the WOA-based MPPT control can be attributed to the selected probabilistic value (p), which can lead to inconsistent or less precise convergence to the MPP. Unlike the GWO algorithm, which updates the position based on the three best solutions (α, β, and δ), the WOA typically focuses only on the best solution found through iterations. This single-point guidance can result in oscillations. The relationship between the turbine output power (Pm) for each algorithm at different wind speeds is shown in Figure 12.

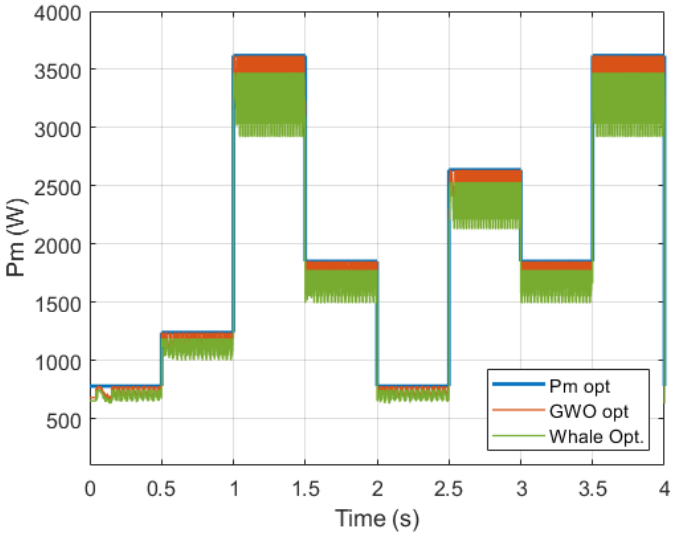

Figure 12. Output Power variations for both algorithms.

In Figure 12, the maximum output power obtained by the GWO-based MPPT control exhibited higher stability and tracked the rated-power curve more efficiently. Compared with the WOA-based MPPT controller, the GWO-based controller demonstrated lower oscillation levels, faster convergence, and higher tracking efficiency in all comparisons, indicating a more stable response under dynamic conditions.

A key aspect of evaluating the selected algorithms is benchmarking their performance against other non-optimization-based MPPT methods widely reported in the literature. Table 2 presents a detailed comparison summary of the different MPPT techniques based on criteria such as the power coefficient, convergence time, tracking efficiency, and oscillation percentage.

The tracking efficiency of the MPPT controller is defined as follows:

$$\eta_{Track}(\%) = \frac{P_{MPPT}(t)}{P_{MAX}(t)} \quad (28)$$

Where $P_{MPPT}(t)$ represents the instant output power obtained by the MPPT controller and $P_{MAX}(t)$ denotes the theoretical maximum power point of the WECS. In Table 2, the WOA method has more oscillations than the GWO method, which lowers the conversion efficiency and degraded performance in the evaluated metrics. Compared to techniques such as Perturb and Observe (P&O) and Fuzzy Logic Controller (FLC), optimization-based methods exhibit superior performance across nearly all metrics, including enhanced tracking accuracy, faster convergence times, and reduced steady-state oscillation. These results make optimization-based methods more robust to nonlinearities, parameter variations, and uncertain wind profiles than conventional methods.

Table 2. Comparison summary of the MPPT optimization algorithms.

MPPT Controls	Power Coefficient	Convergence time (s)	Tracking efficiency	Oscillation percentage
GWO	0.471	0.12	98.2%	<2%
WOA	0.442	0.14	90.4%	<10%
P&O Method [9]	0.39	0.22	78.3%	<22%
FLC Method [18]	0.41	0.17	82.1%	<18%

4. Conclusion

This study presents a comparative analysis of two optimization-based MPPT controllers for a WECS using MATLAB/Simulink. The MPPT controllers aim to maximize energy harvesting by regulating the system converter. The performance of both algorithms was comparatively evaluated under a variable wind speed profile. The numerical results demonstrate that both optimization algorithms effectively tracked the maximum power point under varying wind conditions. However, the GWO-based approach outperformed WOA by achieving a higher power coefficient (0.471) and a shorter convergence time (0.12 s), whereas WOA reached a power coefficient of (0.442) with a convergence time of (0.14 s). In addition, the tracking efficiency of the GWO-based controller reached 98.2%, compared to 90.4% obtained with the WOA method. Another important performance indicator is the oscillation level, where the GWO algorithm maintains oscillations below 2%. The performance fluctuations of WOA-based MPPT control are mainly associated with the probabilistic parameter (p), which

may affect decision consistency under rapidly varying operating conditions. In future research, the proposed algorithms can be evaluated through hardware implementation under multiple wind scenarios to assess their robustness. Furthermore, future research should focus on developing hybrid optimization strategies that integrate complementary optimization techniques to overcome the limitations of single-algorithm approaches and enhance the adaptability and reliability of MPPT systems under dynamic operating conditions.

Acknowledgment

This study was supported by the Scientific Research Projects Coordination Unit of Firat University. Project Number: MF.24.75.

References

1. Maurya V K. Comparative Study of Different Grid Connected Wind Energy Conversion System Configurations. *Journal of Informatics Electrical and Electronics Engineering (JIEEE)* 2021; 2: 1-13. https://doi.org/10.54060/jieee/002.02.024.
2. Mir M, Shafieezadeh M, Heidari M A, et al. Application of hybrid forecast engine based intelligent algorithm and feature selection for wind signal prediction. *Evolving Systems* 2020; 11: 559-73. https://doi.org/10.1007/s12530-019-09271-y.
3. Malik MZ, Baloch MH, Gul M, Kaloi GS, Chauhdary ST, Memon AA. A research on conventional and modern algorithms for maximum power extraction from wind energy conversion system: a review. *Enviromental Science and Pollution Research* 2021; 28: 5020-35. https://doi.org/10.1007/s11356-020-11558-6.
4. Ahmed J, Salam Z. An improved perturb and observe (P&O) maximum power point tracking (MPPT) algorithm for higher efficiency. *Applied Energy* 2015; 150: 97–108. https://doi.org/10.1016/j.apenergy.2015.04.006.
5. Ganjefar S, Ghassemi AA, Ahmadi MM. Improving efficiency of two-type maximum power point tracking methods of tip-speed ratio and optimum torque in wind turbine system using a quantum neural network. *Energy* 2014; 67: 444-53. https://doi.org/10.1016/j.energy.2014.02.023.
6. Nasiri M, Milimonfared J, Fathi SH. Modeling, analysis and comparison of TSR and OTC methods for MPPT and power smoothing in permanent magnet synchronous generator-based wind turbines. *Energy Conversion and Management* 2014; 86: 892-900. https://doi.org/10.1016/j.enconman.2014.06.055.
7. Yokoyama H, Tatsuta F, Nishikata S. Tip speed ratio control of wind turbine generating system connected in series. *2011 International Conference on Electrical Machines and Systems*, Beijing, China: IEEE; 2011, p. 1-4. https://doi.org/10.1109/ICEMS.2011.6073595.
8. Li DY, Song YD, Gan ZX, Cai WC. Fault-Tolerant Optimal Tip-Speed-Ratio Tracking Control of Wind Turbines Subject to Actuation Failures. *IEEE Transactions on Industrial Electronics* 2015; 62(12): 7513-23. https://doi.org/10.1109/TIE.2015.2458968.
9. Mahmoud MS, Oyedeji MO. Adaptive and predictive control strategies for wind turbine systems: a survey. *IEEE/CAA Journal of Automatica Sinica* 2019; 6(2): 364-78. https://doi.org/10.1109/JAS.2019.1911375.
10. Mousa HHH, Youssef A-R, Mohamed EEM. State of the art perturb and observe MPPT algorithms based wind energy conversion systems: A technology review. *International Journal of Electrical Power & Energy Systems* 2021; 126:106598. https://doi.org/10.1016/j.ijepes.2020.106598.
11. Dursun EH, Kulaksiz AA. MPPT Control of PMSG Based Small-Scale Wind Energy Conversion System Connected to DC-Bus. *International Journal of Emerging Electric Power Systems* 2020; 21: 20190188. https://doi.org/10.1515/ijeeps-2019-0188.
12. Pande J, Nasikkar P, Kotecha K, Varadarajan V. A . A Review of Maximum Power Point Tracking Algorithms for Wind Energy Conversion Systems. *Journal of Marine Science and Engineering* 2021; 9(11): 1187. https://doi.org/10.3390/jmse9111187.
13. Apata O, Oyedokun DTO. An overview of control techniques for wind turbine systems. *Scientific African* 2020; 10: e00566. https://doi.org/10.1016/j.sciaf.2020.e00566.
14. Umar DA, Alkawsi G, Jailani NLM, Alomari MA, Baashar Y, Alkahtani AA, Capretz LF, Tiong SK. Evaluating the Efficacy of Intelligent Methods for Maximum Power Point Tracking in Wind Energy Harvesting Systems. *Processes* 2023; 11(5): 1420. https://doi.org/10.3390/pr11051420.
15. Zhang X, Jia J, Zheng L, Yi W, Zhang Z. Maximum power point tracking algorithms for wind power generation system: Review, comparison and analysis. *Energy Science & Engineering* 2023; 11: 430-444. https://doi.org/10.1002/ese3.1313.

16. Vigneswaran K, Suresh Kumar P. Maximum Power Point Tracking (MPPT) Method in Wind Power System. *International Journal of Innovative Research in Science, Engineering and Technology* 2007; 3297: 680-687. https://doi.org/10.15680/IJIRSET.2015.0501118.
17. Chen Z, Li H. Overview of different wind generator systems and their comparisons. *IET Renewable Power Generation* 2008; 2: 123-138. https://doi.org/10.1049/iet-rpg:20070044.
18. Rajvikram M, Renuga P, Swathisriranjani M. Fuzzy based MPPT controller's role in extraction of maximum power in wind energy conversion system. *2016 International Conference on Control, Instrumentation, Communication and Computational Technologies (ICCICCT)*, Kumaracoil, India: IEEE; 2016, p. 713-9. https://doi.org/10.1109/ICCICCT.2016.7988045.
19. Zebraoui O, Bouzi M. Comparative study of different MPPT methods for wind energy conversion system. *IOP Conference Series: Earth and Environmental Science* 2018; 161: 012023. https://doi.org/10.1088/1755-1315/161/1/012023.
20. Thongam JS, Bouchard P, Ezzaidi H, Ouhrouche M. Artificial neural network-based maximum power point tracking control for variable speed wind energy conversion systems. *2009 IEEE International Conference on Control Applications*, St. Petersburg, Russia: IEEE; 2009, p. 1667-71. https://doi.org/10.1109/CCA.2009.5281181.
21. Belmokhtar K, Doumbia ML, Agbossou K. Novel fuzzy logic based sensorless maximum power point tracking strategy for wind turbine systems driven DFIG (doubly-fed induction generator). *Energy* 2014; 76: 679-93. https://doi.org/10.1016/j.energy.2014.08.066.
22. Wei C, Zhang Z, Qiao W, Qu L. An Adaptive Network-Based Reinforcement Learning Method for MPPT Control of PMSG Wind Energy Conversion Systems. *IEEE Transactions on Power Electronics* 2016; 31: 7837-7848. https://doi.org/10.1109/TPEL.2016.2514370.
23. Qais MH, Hasanien HM, Alghuwainem S. Enhanced whale optimization algorithm for maximum power point tracking of variable-speed wind generators. *Applied Soft Computing Journal* 2020; 86: 105937. https://doi.org/10.1016/j.asoc.2019.105937.
24. Muñoz-Palomeque E, Sierra-García JE, Santos M. Wind turbine maximum power point tracking control based on unsupervised neural networks. *Journal of Computational Design and Engineering* 2023; 10:108-121. https://doi.org/10.1093/jcde/qwac132.
25. Sayeh KF, Tamalouzt S, Ziane D, Bekhiti A, Belkhier Y. Utilizing Fuzzy Logic Control and Neural Networks Based on Artificial Intelligence Techniques to Improve Power Quality in Doubly Fed Induction Generator‐Based Wind Turbine System. *International Journal of Energy Research* 2025; 2025: 5985904. https://doi.org/10.1155/er/5985904.
26. Roummani K, Ferroudji F, Saihi L, Koussa K. Grey Wolf Optimization Based MPPT Control of Grid Connected Direct Driven Wind Energy Conversion System. *Proceedings of the 1st International Conference on Advanced Renewable Energy Systems*, Singapore: Springer Nature Singapore; 2024, p. 483-92. https://doi.org/10.1007/978-981-99-2777-7_53.
27. Qais MH, Hasanien HM, Alghuwainem S, Nouh AS. Coyote optimization algorithm for parameters extraction of three-diode photovoltaic models of photovoltaic modules. *Energy* 2019; 187: 116001. https://doi.org/10.1016/j.energy.2019.116001.
28. Jung M-A, Lee Y. Performance Comparisons of Bio-Inspired Optimization Algorithms for Grid Synchronization. *Korean Journal of Artificial Intelligence* 2025; 13:23-29. https://doi.org/10.24225/kjai.2025.13.2.23.
29. Hasan A, Yaqoob Javed M, Shahid K, Mussenbrock T. Optimized Maximum Power Point Tracking for Hybrid PV-TEG Systems Using an Improved Water Cycle Algorithm. *IEEE Access* 2025; 13: 149343-149360. https://doi.org/10.1109/ACCESS.2025.3601440.
30. Zhang H, Liu Y, Jing T, Lu C. Adaptive MPPT Algorithm Based on Grey Wolf Optimization for Photovoltaic Systems in Dynamic Weather Conditions. *2025 3rd International Conference on Power, Grid and Energy Storage*, Chengdu, China: IEEE; 2025, p. 487-90. https://doi.org/10.1109/PGES66344.2025.11193432.
31. Makhadmeh SN, Kassaymeh S, Rjoub G, Bataineh B, Sanjalawe Y, Al-Betar MA. Recent advances in multi-objective whale optimization algorithm, its versions and applications. *Journal of King Saud University Computer and Information Sciences* 2025; 37: 200. https://doi.org/10.1007/s44443-025-00184-2.
32. Ali M, Garip I, Colak I. Improved Cuckoo Search Algorithm for Wind System Optimization. *2022 10th International Conference on Smart Grid (icSmartGrid)*, Istanbul, Turkey: IEEE; 2022, p. 431-5. https://doi.org/10.1109/icSmartGrid55722.2022.9848713.
33. Fathy A, Alharbi AG, Alshammari S, Hasanien HM. Archimedes optimization algorithm based maximum power point tracker for wind energy generation system. *Ain Shams Engineering Journal* 2022; 13(2): 101548. https://doi.org/10.1016/j.asej.2021.06.032.
34. Sridharan S, Vasan VP, Velmurugan P. Efficient maximum power point tracking in grid connected switched reluctance generator in wind energy conversion system: an enhanced Mayfly Algorithm transient search optimization. *Energy Sources, Part A: Recovery, Utilization, and Environmental Effects* 2025; 47: 6812-6829. https://doi.org/10.1080/15567036.2021.2008059.

35. Benkercha R, Moulahoum S, Colak I. Modelling of Fuzzy Logic Controller of a Maximum Power Point Tracker Based on Artificial Neural Network. *2017 16th IEEE International Conference on Machine Learning and Applications (ICMLA)*, Cancun, Mexico: IEEE; 2017, p. 485-92. https://doi.org/10.1109/ICMLA.2017.0-114.
36. Kumar D, Chatterjee K. A review of conventional and advanced MPPT algorithms for wind energy systems. *Renewable and Sustainable Energy Reviews* 2016; 55: 957-970. https://doi.org/10.1016/j.rser.2015.11.013.
37. Sathasivam K, Garip I, Saeed SH, Yais Y, Alanssari AI, Hussein AA, Hammoode JA, Lafta AM. A Novel MPPT Method Based on PSO and ABC Algorithms for Solar Cell. *Electric Power Components and Systems* 2024; 52: 653-664. https://doi.org/10.1080/15325008.2023.2228795.
38. Zhang L, Wang S, Ni Z, Li F. Maximum power point tracking control of photovoltaic systems using a hybrid improved whale particle swarm optimization algorithm. *Energy Sources, Part A: Recovery, Utilization, and Environmental Effects* 2025; 47: 1789-1803. https://doi.org/10.1080/15567036.2024.2448157.
39. Hussan U, Waheed A, Bilal H, Wang H, Hassan M, Ullah I, Peng J, Hosseinzadeh M. Robust Maximum Power Point Tracking in PV Generation System: A Hybrid ANN-Backstepping Approach With PSO-GA Optimization. *IEEE Transactions on Consumer Electronics* 2025; 71: 6016-6026. https://doi.org/10.1109/TCE.2025.3569871.
40. Karimi H, Siadatan A, Rezaei-Zare A. A Hybrid P&O-Fuzzy-Based Maximum Power Point Tracking (MPPT) Algorithm for Photovoltaic Systems Under Partial Shading Conditions. *IEEE Access* 2025; 13: 86046-86056. https://doi.org/10.1109/ACCESS.2025.3533314.
41. Rashmi G, Linda MM. A novel MPPT design for a wind energy conversion system using grey wolf optimization. *Automatika* 2023; 64: 798-806. https://doi.org/10.1080/00051144.2023.2218168.
42. Alhamdawee R, Hussain MM. A study of conventional and modern algorithms employed for MPPT in wind energy conversion systems: A review. *2024 3rd International conference on Power Electronics and IoT Applications in Renewable Energy and its Control (PARC)*, Mathura, India: IEEE; 2024, p. 14-23. https://doi.org/10.1109/PARC59193.2024.10486569.
43. Hai T, Zhou J, Dadfar S. A novel intelligent method to increase accuracy of hybrid photovoltaic-wind system-based MPPT and pitch angle controller. *Soft Computing* 2023 2023: 1-18. https://doi.org/10.1007/S00500-023-07977-5.
44. Vardia M, Priyadarshi N, Ali I, Azam F, Bhoi AK. Maximum Power Point Tracking for Wind Energy Conversion System. In: Advances in Greener Energy Technologies, Singapore: Springer Singapore; 2020, p. 631-40. https://doi.org/10.1007/978-981-15-4246-6_36.
45. Ackermann T. *Wind Power in Power Systems*. Chichester, UK: John Wiley & Sons, Ltd; 2005. https://doi.org/10.1002/0470012684.
46. Yazıcı İ, Yaylacı EK, Cevher B, Yalçın F, Yüzkollar C. A new MPPT method based on a modified Fibonacci search algorithm for wind energy conversion systems. *Journal of Renewable and Sustainable Energy* 2021; 13: 013304. https://doi.org/10.1063/5.0035134.
47. Mostafa M, El-Hay EA, Elkholy MM. Chapter 6: Recent maximum power point tracking methods for wind energy conversion system. In: Energy Efficiency of Modern Power and Energy Systems, Elsevier; 2024, p. 101-22. https://doi.org/10.1016/B978-0-443-21644-2.00006-3.
48. Perçin HB, Çalışkan A. Archimedes Optimization Algorithm-Based Pitch Angle Control In Wind Energy Systems. *Middle East Journal of Science* 2024; 10: 151-166. https://doi.org/10.51477/mejs.1591919.
49. Teklehaimanot YK, Akingbade FK, Ubochi BC, Ale TO. A review and comparative analysis of maximum power point tracking control algorithms for wind energy conversion systems *International Journal of Dynamics and Control* 2024. https://doi.org/10.1007/s40435-024-01434-3.
50. Anaya Lara O, Jenkins N, Ekanayake J, Cartwright P, Hughes M. *Wind Energy Generation Systems: Modelling and Control* Chichester, UK: John Wiley & Sons, Ltd; 2009.
51. Wu B, Lang Y, Zargari N, Kouro S. *Power Conversion and Control of Wind Energy Systems.* Hoboken, NJ, USA: John Wiley & Sons, Inc.; 2011. https://doi.org/10.1002/9781118029008.
52. Mirjalili S, Mirjalili SM, Lewis A. Grey Wolf Optimizer. *Advances in Engineering Software* 2014; 69: 46-61. https://doi.org/10.1016/j.advengsoft.2013.12.007.
53. Ali YA, Ouassaid M. Sensorless MPPT Controller using Particle Swarm and Grey Wolf Optimization for Wind Turbines. *2019 7th International Renewable and Sustainable Energy Conference (IRSEC)*, vol. 2, IEEE; 2019, p. 1-7. https://doi.org/10.1109/IRSEC48032.2019.9078151.

54. Mohamed AAA, Haridy AL, Hemeida AM. The Whale Optimization Algorithm based controller for PMSG wind energy generation system. *Proceedings of 2019 International Conference on Innovative Trends in Computer Engineering, ITCE 2019*, IEEE; 2019, p. 438-43. https://doi.org/10.1109/ITCE.2019.8646353.
55. Percin HB, Caliskan A. Whale optimization algorithm based MPPT control of a fuel cell system. *International Journal of Hydrogen Energy* 2023; 48: 23230-23241. https://doi.org/10.1016/j.ijhydene.2023.03.180.
56. Abbadi A, Hamidia F, Skender MR, Bettache F. Grey Wolf MPPT Controller for Grid Connected Residential Wind System Operating Under Low and High Variations. In: Wind Speed, Springer, Cham; 2023, p. 261-268. https://doi.org/10.1007/978-3-031-21216-1_28.
57. Abed Hannon HA, Latif HK, Abdulsadda AT. Archimedes optimization algorithm based grey wolf optimizer to achieve maximum power point tracking for enhancing performance and efficiency of photovoltaic systems, *AIP Conference Proceedings* 2023, p. 050041. https://doi.org/10.1063/5.0162048.